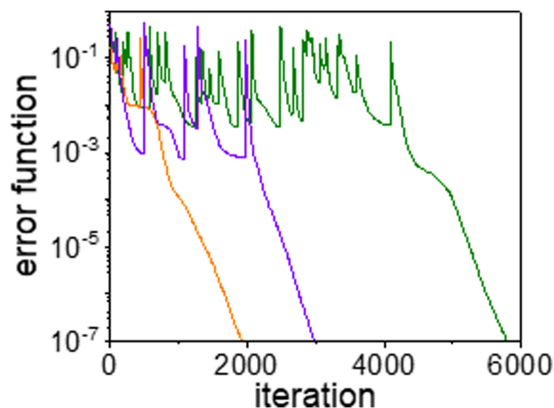
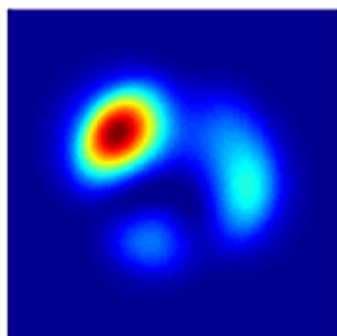


High-Precision Modal Decomposition of Laser Beams Based on Globally Optimized SPGD Algorithm

Volume 11, Number 5, October 2019

Kyuhong Choi
Changsu Jun



DOI: 10.1109/JPHOT.2019.2937125

High-Precision Modal Decomposition of Laser Beams Based on Globally Optimized SPGD Algorithm

Kyuhong Choi  and Changsu Jun 

Advanced Photonics Research Institute, Gwangju Institute of Science and Technology,
Gwangju 61005, South Korea

DOI:10.1109/JPHOT.2019.2937125

This work is licensed under a Creative Commons Attribution 4.0 License. For more information, see <https://creativecommons.org/licenses/by/4.0/>

Manuscript received April 29, 2019; revised August 6, 2019; accepted August 20, 2019. Date of publication August 23, 2019; date of current version September 6, 2019. This work was supported in part by the MOTIE & DAPA of South Korea (UM16211RD2) and in part by the ADD of South Korea (UD180040ID). Corresponding author: Changsu Jun (e-mail: changsu.jun@gist.ac.kr).

Abstract: We propose a globally optimized stochastic parallel gradient descent (SPGD) algorithm to analyze the modal content of laser beams with high precision. Modal decomposition (MD) based on conventional SPGD algorithms often falls to a local minimum when a laser beam consists of six or more fiber eigenmodes, which results in a false combination of modes. While keeping the simplicity and speed advantages of the SPGD algorithm, we adopted several optimization techniques to discern the global minimum from local minima and achieve better accuracy. The enhanced SPGD algorithm includes the annealing of the learning rates, identifying and escaping of local minima with large perturbations, and comparing of the transient error function with a reference value. We were able to exactly analyze the modal content of beams from six-mode optical fibers with high precision in seconds. Calculation of the modal weight and phase percentage errors, as well as simulations of far-field evolution images, confirmed the importance of finding the global minimum in improving the accuracy and real-time analysis of MD. The simple structure of the enhanced algorithm and its global optimization ability in multimode fibers will accelerate numerical MD in diverse laser applications.

Index Terms: Modal decomposition, SPGD algorithm, fiber laser, global minimum.

1. Introduction

As laser performance and applications evolve, analyzing and assessing beam quality is becoming correspondingly important. For this, beam profile and M^2 value are the traditional metrics. However, exact modal content—including modal weights and phases—is becoming more essential; especially in high-power fiber lasers. In pushing the power limits of fiber lasers [1], large mode area fibers [2] are mandatory to reduce power density and nonlinearity in the fiber core. However, these often excite higher-order modes, leading to transverse mode instability (TMI) [3]. Analyzing the modal content of the output beam is a direct indicator of this TMI [4], [5]. Other applications that utilize the spatial characteristics of laser beams—such as multimode combiners, splitters, and amplifiers for mode-division-multiplexing [6], and spatiotemporally mode-locked fiber lasers [7]—would also benefit from modal decomposition (MD).

Many experimental MD techniques have been proven relevant and precise [8]–[11]. However, experimental techniques require an additional broadband light source and dominant fundamental

mode [8], [9] or delicate optical setup [11]. For example, S^2 [8] imaging requires broadband light source and optical spectrum analyzer to measure the wavelength modulation induced by modal interference. These techniques are often not easily integrated with the main laser system and require additional time for experimentation and analysis. Modal decomposition can be based on wavefront sensor and it can provide complex amplitude of laser beams [10], [12]. Especially, MD only based on beam profile attracts much attention because it can be faster (or even real-time) and accurate. The Gerchberg-Saxton [13], [14], stochastic parallel gradient descent (SPGD) [5], [15], and genetic algorithm [16] have been widely studied. In these numerical methods, the reconstructed beam profile—which is a linear combination of each eigenmode—is iteratively compared with the input beam to find the most probable MD solution or to minimize the error function between the two. In cases where the laser beam consists of three fiber eigenmodes, iterative reconstruction with random initial conditions always converges on one solution. This means there is only one combination that looks exactly like the input beam [15]. However, six or more fiber eigenmodes present a difficulty in the form of the local minimum problem. Besides the exact solution—which is called the global minimum—there can be several other local minima that result in a very similar beam profile but are false modal combinations [16]. Therefore, to make optimal use of numerical MD and apply it to a real beam in real time, accuracy should be guaranteed by first resolving the local minimum problem. Recently, a hybrid genetic algorithm combined with SPGD was suggested as a method to globally optimize the MD iteration, but the calculation takes hundreds of seconds [16]. A convolutional neural network-based approach [17] was also introduced. However, several questions—such as how to discern local and global minima and how small of an error function is acceptable—have not yet been answered. Understanding these basic questions can lead to an alternate solution for a simple, fast, and accurate numerical MD method.

In this work, we investigate how to globally optimize numerical MD. After pre-studying the convergence behaviors of local and global minima based on a conventional SPGD algorithm, we set a reference value—either a critical value for the global minimum or a target value smaller than the critical value for better accuracy. In the modified SPGD loop, a local minimum escaping step was added. Subsequently, the loop iterates until the reference value is reached. These techniques are often used in machine learning and we adopted them for modal decomposition in this work. With rigorous analysis and the globally optimized SPGD algorithm, any random initial conditions can converge on the global minimum for up to six modes based on the near-field beam profile. We verified the modified algorithm with numerous beam combinations, and an error function as small as 10^{-7} was acquired. Moreover, far-field evolutions of generated, reconstructed local- and global-minimum beams were crosschecked. The algorithm is based only on near-field images, and therefore phase ambiguity due to conjugate pairs still exists. In applications where phase ambiguity needs to be resolved, the true phase can be found just by comparing the far-field evolution image with the measured one. The enhanced SPGD algorithm can also be applied to beams in which a higher number of eigenmodes are superposed.

2. Globally Optimized SPGD Algorithm

Numerical MD used is to find the modal weight and phase of each eigenmode constituting the input beam profile (or the measured one). For this, we assume the beam is from a multimode optical fiber. Calculation starts with reconstructing the beam as a linear combination of each mode:

$$U(x, y) = \sum_{j=1}^N \rho_j e^{i\phi_j} \psi_j(x, y) \quad (1)$$

where $U(x, y)$ is the total amplitude of N modes; ρ_j^2 and ϕ_j are the modal weight and phase of j th mode, respectively; and $\psi_j(x, y)$ is the normalized amplitude of each linearly polarized (LP) mode. The total beam intensity distribution $I(x, y)$ is as follows:

$$I(x, y) = |U(x, y)|^2 \quad (2)$$

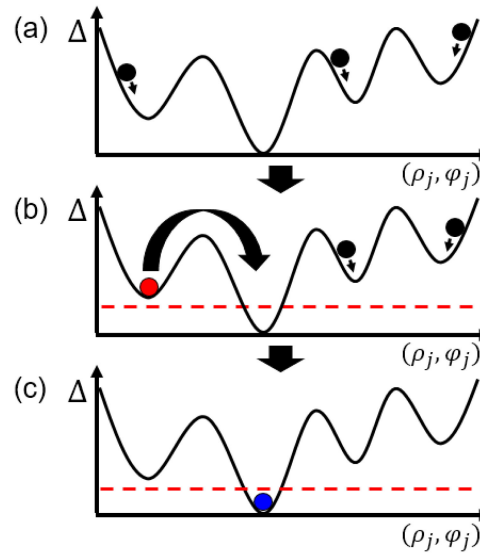


Fig. 1. Schematic diagram of the globally optimized SPGD algorithm.

In the SPGD algorithm, the reconstructed beam profile evolves into the input beam profile by iteratively comparing the shape similarity and updating the perturbation coefficients of each mode. For shape comparison, we usually define a cost function or error function [13] that calculates the normalized product between the measured beam, $I_{me}(x, y)$, and the reconstructed one, $I_{re}(x, y)$.

$$\Delta = 1 - \frac{\iint I_{me}(x, y) I_{re}(x, y) dx dy}{\sqrt{\iint I_{me}^2(x, y) dx dy \iint I_{re}^2(x, y) dx dy}} \quad (3)$$

where Δ is the error function, which is 0 when $I_{me}(x, y) = \alpha I_{re}(x, y)$ (α is a constant). In the process of decreasing the error function using the conventional SPGD algorithm, three-mode cases always find a global minimum, but six-mode cases often fall to local minima. These have similar beam shapes to that of the measured beam in the calculated near-field plane, but far-field propagations result in totally different shapes. The number of local minima is equal to the number of probable linear combinations of each mode that have a similar beam shape to that of the input beam and are not exact solutions. We tried several approaches to avoid the local minima issue: for example, SPGD with multiple initial condition sets or multiple perturbations of different sizes. However, estimating the number of initial condition sets was difficult and the approaches were very time-consuming and ineffective. Eventually, by adding a step to the conventional SPGD algorithm—i.e., identifying a local minimum and escaping from it until the error function reaches the global minimum—the problem could be solved.

Figure 1 shows a diagram of the globally optimized SPGD algorithm. One or a few initial value sets are randomly chosen, and each begins an iteration according to the SPGD algorithm (Fig. 1(a)). Only the smallest error function among them is taken and the algorithm identifies it as a local minimum if a certain number of iterations converge on a plateau (red circle in Fig. 1(b)). To escape from the local minimum, a large perturbation is applied, and the iterations proceed until the reference value threshold (red dotted line) is crossed, which was set below the smallest error function (Fig. 1(c)). Through this procedure, we can find the global optimum.

Figure 2 shows a detailed flowchart of the globally optimized SPGD algorithm. The process is described as follows:

- 1) Generate the initial values, $\{\rho_{j,k}|j = 1, 2, \dots, N\}$ and $\{\varphi_{j,k}|j = 2, 3 \dots, N\}$, where $\varphi_{j,k}$ is the phase difference between the fundamental mode and the j th mode of the k th initial condition set; N is the total number of eigenmodes; and m_1 and m_2 are the learning rates that will decrease

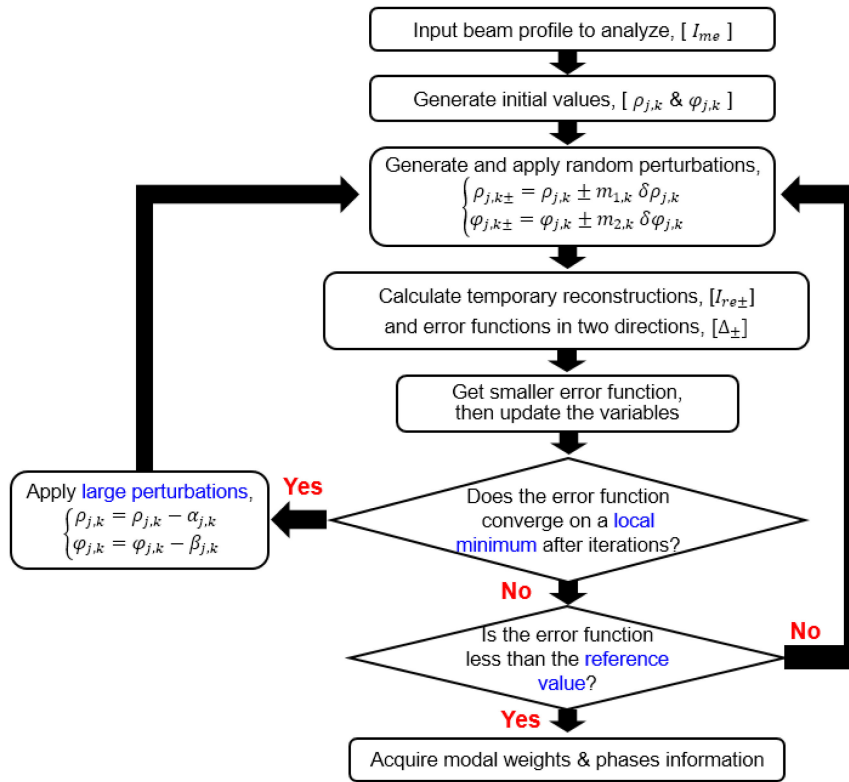


Fig. 2. Globally optimized SPGD algorithm.

logarithmically as the error function approaches zero. The error function is calculated from $2N - 1$ variables.

- 2) Generate and apply the random perturbations, $\delta\rho_{j,k}$ and $\delta\varphi_{j,k}$, and calculate the temporary reconstructions, $I_{re\pm}$, and error functions in two directions, Δ_{\pm} . After acquiring the smaller error function, update the variables using the error function difference, $\delta\Delta = \Delta_+ - \Delta_-$.
- 3) After a certain number of iterations, determine whether the error function converges on a local minimum or not. If yes, apply a perturbation, $\{\alpha_{j,k}, \beta_{j,k}\}$, that is far larger than the initial perturbation, and return to (2).
- 4) If it does not converge on a local minimum, compare the error function to the reference value, which is set below the smallest local minimum. The iterations proceed as long as the error function is larger than the reference value. Once the error function crosses the reference value threshold, we can acquire the modal weights and phases.

In the following section, the convergence behavior of local and global minima based on the conventional SPGD algorithm are studied. Additionally, setting of the reference value for six-mode optical fibers and the subsequent MD results are also described.

3. Simulation Results and Discussion

We verified the globally optimized SPGD algorithm with beams composed of six eigenmodes. The simulation assumed a step-index multimode fiber with a core diameter of $25 \mu\text{m}$ and numerical aperture (NA) of 0.065; thus, the V-number was approximately 4.798 at 1064 nm. The image pixel size was 100×100 and the calculation was performed with an Intel Core i5-8400 at 2.8 GHz and 4 GB memory.

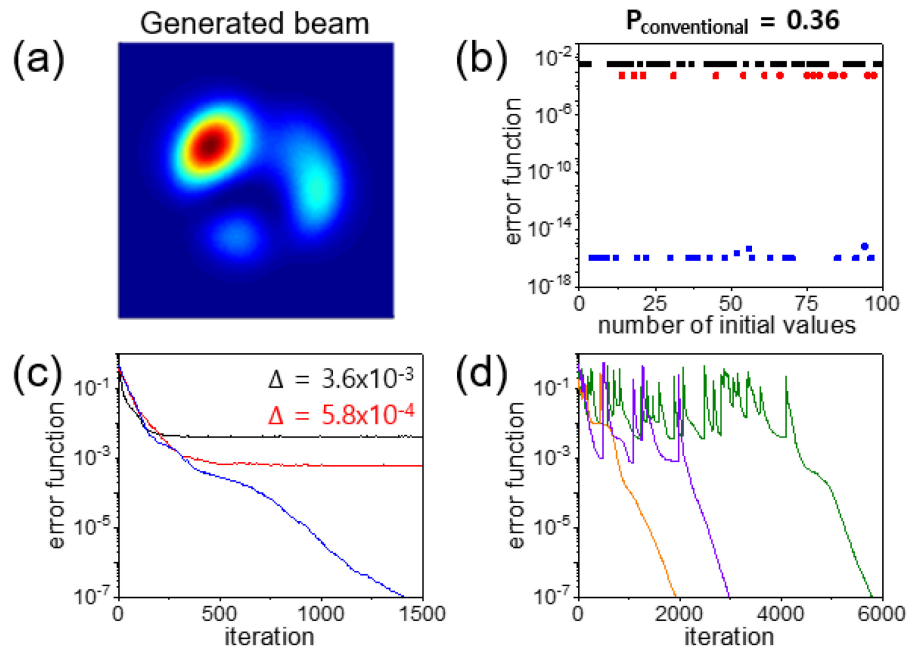


Fig. 3. (a) Generated beam profile to analyze. (b) Error functions under conventional SPGD algorithm for 100 different initial values (black and red data: local minima, blue data: global minimum). Error function evolution per iteration in case of (c) conventional SPGD (Error functions of local minima are denoted in the figure) and (d) the globally optimized SPGD algorithm (Each color means different initial conditions.).

TABLE 1

Modal Content of the Generated Beam and Reconstruction Errors for Three Target Error Functions

		LP ₀₁	LP _{11,o}	LP _{11,e}	LP _{21,o}	LP _{21,e}	LP ₀₂	
Generated beam	ρ^2	0.302	0.235	0.011	0.269	0.144	0.039	
	φ	0	-0.136	-1.700	-2.417	-0.045	-3.054	
reconstruction error	$\Delta = 3.6 \times 10^{-3}$	$\rho_{\text{err}}^2(\%)$	-29.86	-6.64	30.40	1.97	0.43	3.70
		$\varphi_{\text{err}}(\%)$	0	45.52	-11.99	-8.86	-12.89	-22.12
	$\Delta = 5.8 \times 10^{-4}$	$\rho_{\text{err}}^2(\%)$	5.86	-4.74	4.69	-4.64	-3.16	1.99
		$\varphi_{\text{err}}(\%)$	0	13.3	-98.25	49.92	15.34	-1.54
	$\Delta = 1.0 \times 10^{-7}$	$\rho_{\text{err}}^2(\%)$	0.01	0.02	-0.01	-0.03	0.01	0.01
		$\varphi_{\text{err}}(\%)$	0	-0.02	-0.06	-0.03	-0.05	-0.17

In Section 3.1, we study the convergent behaviors of the local and global minima. In Section 3.2, we display the percentage errors of the modal weight and phase according to the error function, and the far-field evolution results of the local and global minima. Lastly, exemplary MD results based on the globally optimized SPGD algorithm are presented and discussed in Section 3.3.

3.1 Comparison Between Conventional and Globally Optimized SPGD Algorithms

Figure 3 and Table 1 show the results of MD based on the globally optimized SPGD algorithm compared to those based on conventional SPGD. Fig. 3(a) depicts a randomly generated beam to be analyzed; its details are found in Table 1. The generated beam plays the role of “input beam” or “measured beam” of the experiment, but is an artificial beam for numerical simulation in this work. First, we studied the convergent behavior of error functions for 100 random initial conditions

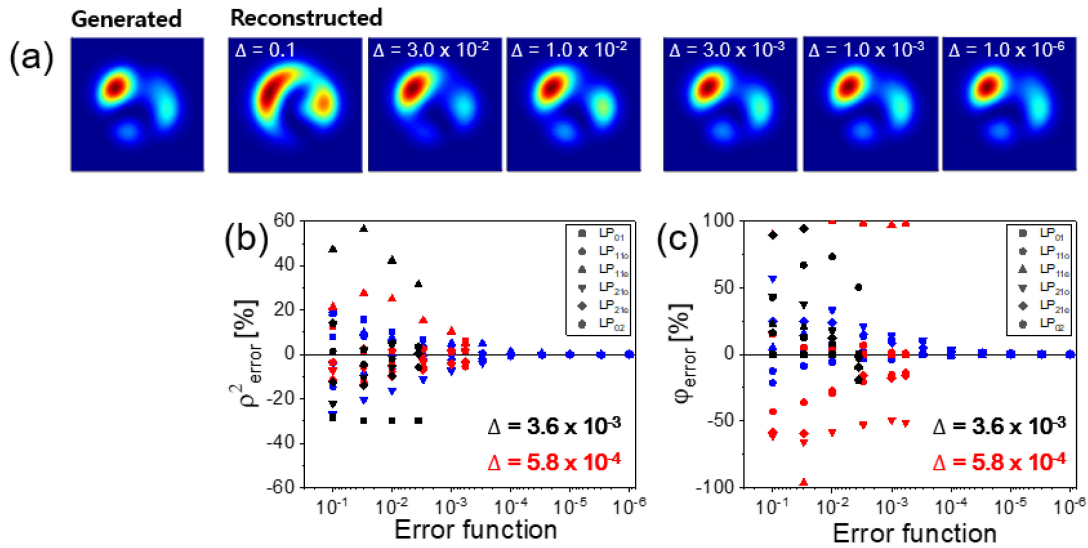


Fig. 4. Beam shapes and modal percentage errors per error function. (a) Generated beam profile (leftmost) and reconstructed beam profile per error function. (b) Modal weight errors and (c) phase difference errors per error function. (black and red data: local minima, blue data: global minimum) Each LP mode is represented with a differently shaped dot.

using the conventional SPGD algorithm, as shown in Fig. 3(b). After more than 10,000 iterations for each initial value, three discrete routes were found. 64% of all cases converged on two local minima with the error functions 3.6×10^{-3} and 5.8×10^{-4} , corresponding to the black and red data, respectively, in Fig. 3(b). The remaining 36% were global minima (blue data), where the error functions monotonically decreased with each iteration. The probability of finding the global minimum among all trials is expressed as $P_{\text{conventional}}$. Examples of evolution per iteration for the three cases are shown in Fig. 3(c). Meanwhile, Fig. 3(d) shows the evolution of the error functions for three random initial conditions based on the globally optimized SPGD algorithm. As explained in Section 2, a large perturbation is applied to the variables to escape a local minimum at each iteration until the reference value is reached. The many spikes in Fig. 3(d) are due to the reset of variables immediately following a large perturbation. The application of large perturbations continues until the algorithm identifies the global minimum. Therefore, any initial values eventually fall to the global minimum, as shown in Fig. 3(d). Practically, only one trace (orange data)—that reaches the global valley first among a few initial conditions—is selected and continues through the iteration. The selected trace (orange data) stops iterating when the error function crosses the reference value that is set as 10^{-7} in Fig. 3(d). Table 1 shows that the modal weight error was less than 0.03% and the phase error was less than 0.2% when globally optimized, while the errors of local minima were as high as 98.25%. Here, the percentage errors of modal weight and phase are calculated as, $\rho^2_{\text{err},j} = (\rho_j^2 - \rho_{re,j}^2) \times 100$, $\varphi_{\text{err},j} = (\varphi_j - \varphi_{re,j})/\pi \times 100$.

3.2 Errors of Local and Global Minima

In Fig. 4, the beam shapes and modal errors are displayed according to the error functions, which are based on the data in Fig. 3 and Table 1. As the error function decreases, the reconstructed beam shape in Fig. 4(a) becomes similar to the generated beam (leftmost). In this example, the error functions down to $\sim 10^{-4}$ belong to local minima. However, the reconstructed beams that belong to the local minima and have the error functions around 10^{-3} already have beam shapes indistinguishable from that of the generated beam. This means that the shape similarity alone does not provide accurate results. The percentage errors of each mode confirm the importance of the global minimum, as shown in Fig. 4(b) and (c). Fig. 4(b) shows the modal weight errors of each

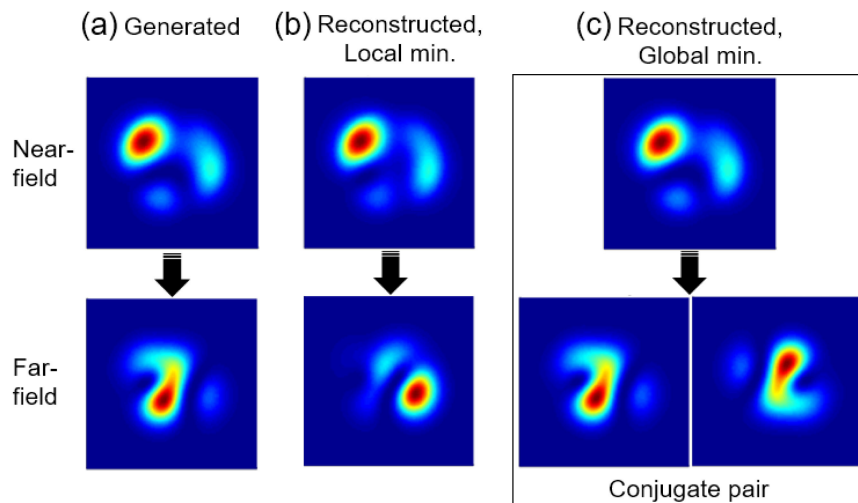


Fig. 5. Near-field beam profiles and far-field evolutions of (a) the generated beam, and the reconstructed beams of (b) a local minimum and (c) the global minimum.

eigenmode per target error function; each eigenmode is represented with a differently shaped dot. For comparison, the data of two local minima and global minimum are overlapped in a graph. Likewise, Fig. 4(c) shows a graph of the phase errors. The errors of the local minima (black and red data) spread out regardless of the error function while the errors of the global minimum (blue data) drastically decrease with the error function.

Far-field evolution [14] confirms how the local and global minima are intrinsically different. In the first row of Fig. 5, we can see the near-field beam shapes of the generated beam (Fig. 5(a)) and reconstructed beams (Fig. 5(b) and (c)), which are seemingly indistinguishable. However, far-field evolution of the local minimum results in the completely different shapes seen in the bottom row of Fig. 5. This is because the modal contents are different. From Figs. 4 and 5, we can see that the shape similarity in the near-field does not alone lead to the solution, while finding the global optimum can only guarantee the exact MD. Though it is globally optimized, the numerical MD is not without phase ambiguity, as shown in Fig. 5(c). This is because the calculations are the same when the phase signs of all modes are opposite in Equation (2). The two beam profiles of the conjugate pair are in origin symmetry in the far-field evolution. As such, for applications in which the phase ambiguity needs to be resolved, the true phase can be found by comparing the far-field evolution image with the measured one.

3.3 MD Results With the Globally Optimized SPGD Algorithm

In the proposed algorithm, setting the reference value is important because it is the criterion to discern between the local and global minima. This value is not derivable theoretically, so it can only be determined statistically. After identifying a local minimum, the reference value to finish the iteration might be set as the value just beneath the error function of the local minimum. However, there could be another local minimum below. Therefore, the smallest local minimum should be identified first to set the reference value. Figure 6 shows the error function distribution of the smallest local minimum for 1000 randomly generated beams. Most of these have values greater than 10^{-6} , while only one has the smallest local minimum of 2.54×10^{-7} . Based on this result, the reference value was set as 10^{-7} for six-mode optical fiber. Alternatively, a smaller value could be chosen for better accuracy. We could not find yet but it can be meaningful if we can express the reference value as functions of any of laser parameters.

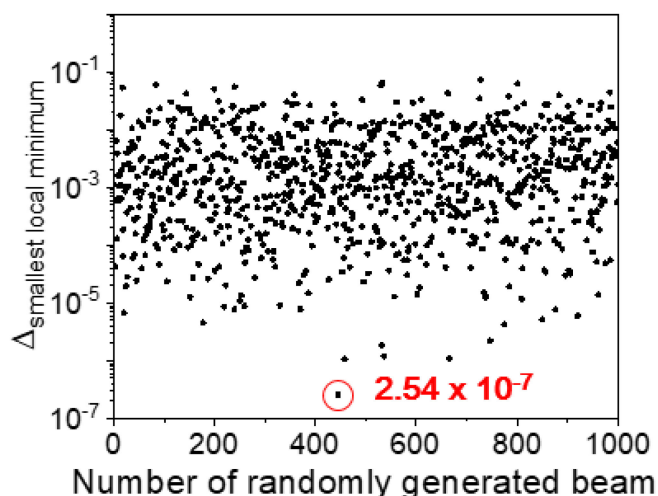


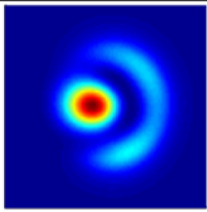
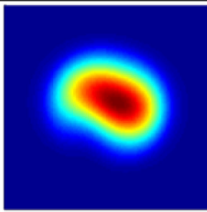
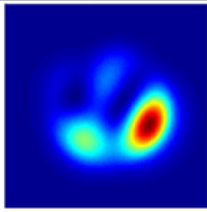
Fig. 6. Error function distribution of the smallest local minimum for 1000 randomly generated beams.

To verify the validity and statistics of the globally optimized SPGD algorithm, we performed simulations with numerous generated beams—three examples are given in Table 2. The error functions were slightly smaller than the reference value of 10^{-7} . Even with such a small target value, the average computation time for beam 1 was 6.05 s at 2944 iterations (100 times averaged), which depends on the initial condition and how quickly the iteration falls into the global valley. The percentage errors were less than 0.4% in all cases. Beams 2 and 3 also showed fast and accurate MD results. While the conventional SPGD cannot be applied to six-mode optical fiber, the modified SPGD algorithm can always find the exact modal content ($P_{globally\ optimized} = 1$) with the additional step of escaping from a local minimum and comparing with the reference value.

As the number of fiber eigenmodes increases, it becomes exceedingly difficult to find the exact modal content by numerical MD due to the local minima problem. The local minima are false combinations of modes that show near-field beam shapes very similar to those of the input beam. The number of local minima is equal to the number of false combinations, and their corresponding error functions represent the degree of similarity in the near-field. The local minima are not true solutions and must be avoided. This is confirmed by the percentage errors per error function and far-field evolutions of the local and global minima. We could also find that exact modal decomposition becomes difficult when a certain eigen-mode takes very low portion in the beam profile.

In this work, we globally optimized the well-known SPGD algorithm by annealing the learning rates and adding the simple step of identifying and escaping local minima. In the process of global optimization, we investigated how to discern the global from a local minimum, and how to set the reference value. In recent studies [16], [17], researchers attempted to reduce the errors of modal weight and phase as much as possible with machine learning algorithms to approach the global minimum. In comparison, in this work, the global minimum was found first to minimize the error function or modal errors. As such, the modified SPGD algorithm in this work can provide high-precision MD in seconds without any complicated algorithm. A preliminary comparison between an i3 and i5 CPU resulted in a difference of approximately 2.5 times in calculation time. In the near future, a higher performing CPU and further optimization for a simpler algorithm will enable real-time analysis, maintaining the feature of global optimization. The proposed algorithm can also be applied to beams in which a higher number of eigenmodes are superposed. It is worth noting that real beam analysis can have many technical issues—for example, resolution of the measured beam profile, beam centering, etc. In such cases, the setting of the reference value may need to be compromised.

TABLE 2
Modal Content of the Generated Beams and the Reconstruction Results of 3 Beams Using the Globally Optimized SPGD Algorithm

		Beam 1	Beam 2	Beam 3			
Generated beams	Beam Profile						
		ρ^2	φ	ρ^2	φ	ρ^2	φ
	LP ₀₁	0.083	0	0.900	0	0.133	0
	LP _{11,o}	0.006	-2.777	0.024	-0.456	0.222	-2.745
	LP _{11,e}	0.374	2.220	0.015	0.707	0.153	1.250
	LP _{21,o}	0.017	-2.920	0.016	-2.510	0.203	-1.237
	LP _{21,e}	0.063	-1.759	0.024	-0.841	0.135	1.339
LP ₀₂	0.457	-1.374	0.021	1.728	0.154	-2.327	
Reconstruction Results (100 times averaged)	$\Delta_{average}$	9.90x10 ⁻⁸		9.93x10 ⁻⁸		9.81x10 ⁻⁸	
	$t_{average}$	6.05s [2.40s~29.57s]		10.04s [4.93s~26.53s]		3.39s [1.37s~9.86s]	
	$N_{iteration, average}$	2944 [1284~12932]		4565 [2241~12069]		1752 [709~5093]	
	$ \rho_{err}^2 $	< 0.07%		< 0.05%		< 0.06%	
	$ \varphi_{err} $	< 0.16%		< 0.40%		< 0.08%	
	$P_{conventional}$	0.58		0.49		0.23	
	$P_{globally optimized}$	1		1		1	

4. Conclusions

A globally optimized SPGD algorithm was proposed and demonstrated fast and accurate MD results based on near-field images from a six-mode optical fiber. A conventional SPGD algorithm can analyze modal content well enough in three-mode optical fiber but has difficulty in six or more modes because of the local minimum issue. By adding procedures for identifying and escaping a local minimum and comparing the transient error function with a reference value, we could precisely analyze the modal content of beams from six-mode optical fibers with high precision. We investigated how to discern local minima from the global minimum, and how to set a reference value for better accuracy. With the aforementioned analysis and globally optimized SPGD algorithm, any random initial conditions can converge on the global minimum based on the near-field beam profile in seconds. Calculation of the percentage errors and far-field evolution emphasized the importance of finding the global minimum first. This globally optimized SPGD algorithm can be applied to a greater number of modes and real-time, real-beam analysis. Furthermore, laser active optimization and coherent beam combining would also benefit from this enhanced SPGD algorithm.

References

- [1] M. N. Zervas and C. A. Codemard, "High-power fiber lasers: A review," *IEEE J. Sel. Top. Quantum Electron.*, vol. 20, no. 5, 2014, Art. no. 0904123.
- [2] N. G. R. Broderick, H. L. Offerhaus, D. J. Richardson, R. A. Sammut, J. Caplen, and L. Dong, "Large mode area fibers for high power applications," *Opt. Fiber Technol.*, vol. 5, no. 2, pp. 185–196, 1999.

- [3] A. V. Smith and J. J. Smith, "Mode instability in high power fiber amplifiers," *Opt. Exp.*, vol. 19, no. 11, pp. 10180–10192, 2011.
- [4] F. Stutzki *et al.*, "High-speed modal decomposition of mode instabilities in high-power fiber lasers," *Opt. Lett.*, vol. 36, pp. 4572–4574, 2011.
- [5] L. Huang *et al.*, "Mode instability dynamics in high-power low-numerical-aperture step-index fiber amplifier," *Appl. Opt.*, vol. 56, pp. 5412–5417, 2017.
- [6] Z. Zhang *et al.*, "21 spatial mode erbium-doped fiber amplifier for mode division multiplexing transmission," *Opt. Lett.*, vol. 43, no. 7, pp. 1550–1553, 2018.
- [7] L. G. Wright, D. N. Christodoulides, and F. W. Wise, "Spatiotemporal mode-locking in multimode fiber laser," *Science*, vol. 358, no. 6359, pp. 94–97, 2017.
- [8] J. W. Nicholson, A. D. Yablon, J. M. Fini, and M. D. Mermelstein, "Measuring the modal content of large-mode-area fibers," *IEEE J. Sel. Topics Quantum Electron.*, vol. 15, no. 1, pp. 61–70, Jan. 2009.
- [9] D. N. Schimpf, R. A. Barankov, and S. Ramachandran, "Cross-correlated (C2) imaging of fiber and waveguide modes," *Opt. Exp.*, vol. 19, no. 14, pp. 13008–13019, 2011.
- [10] M. Paurisse, L. Leveque, M. Hanna, F. Druon, and P. Georges, "Complete measurement of fiber modal content by wavefront analysis," *Opt. Exp.*, vol. 20, no. 4, pp. 4074–4084, 2012.
- [11] Y. Z. Ma *et al.*, "Fiber-modes and fiber-anisotropy characterization using low-coherence interferometry," *Appl. Phys. B*, vol. 96, pp. 345–353, 2009.
- [12] J. Ko and C. C. Davis, "Comparison of the plenoptic sensor and the Shack–Hartmann sensor," *Appl. Opt.*, vol. 56, pp. 3689–3698, 2017.
- [13] R. Brüning, P. Gelszinnis, C. Schulze, D. Flamm, and M. Duparré, "Comparative analysis of numerical methods for the mode analysis of laser beams," *Appl. Opt.*, vol. 52, no. 32, pp. 7769–7777, 2013.
- [14] O. Shapira, A. F. Abouraddy, J. D. Joannopoulos, and Y. Fink, "Complete modal decomposition for optical waveguides," *Phys. Rev. Lett.*, vol. 94, pp. 143902–143905, 2005.
- [15] L. Huang, S. Guo, J. Leng, H. Lü, P. Zhou, and X. Cheng, "Real-time mode decomposition for few-mode fiber based on numerical method," *Opt. Exp.*, vol. 23, no. 4, pp. 4620–4629, 2015.
- [16] L. Li, J. Leng, P. Zhou, and J. Chen, "Multimode fiber modal decomposition based on hybrid genetic global optimization algorithm," *Opt. Exp.*, vol. 25, no. 17, pp. 19680–19690, 2017.
- [17] Y. An, L. Huang, J. Li, J. Leng, L. Yang, and P. Zhou, "Learning to decompose the modes in few-mode fibers with deep convolutional neural network," *Opt. Exp.*, vol. 27, pp. 10127–10137, 2019.